Suppl. Figure 1

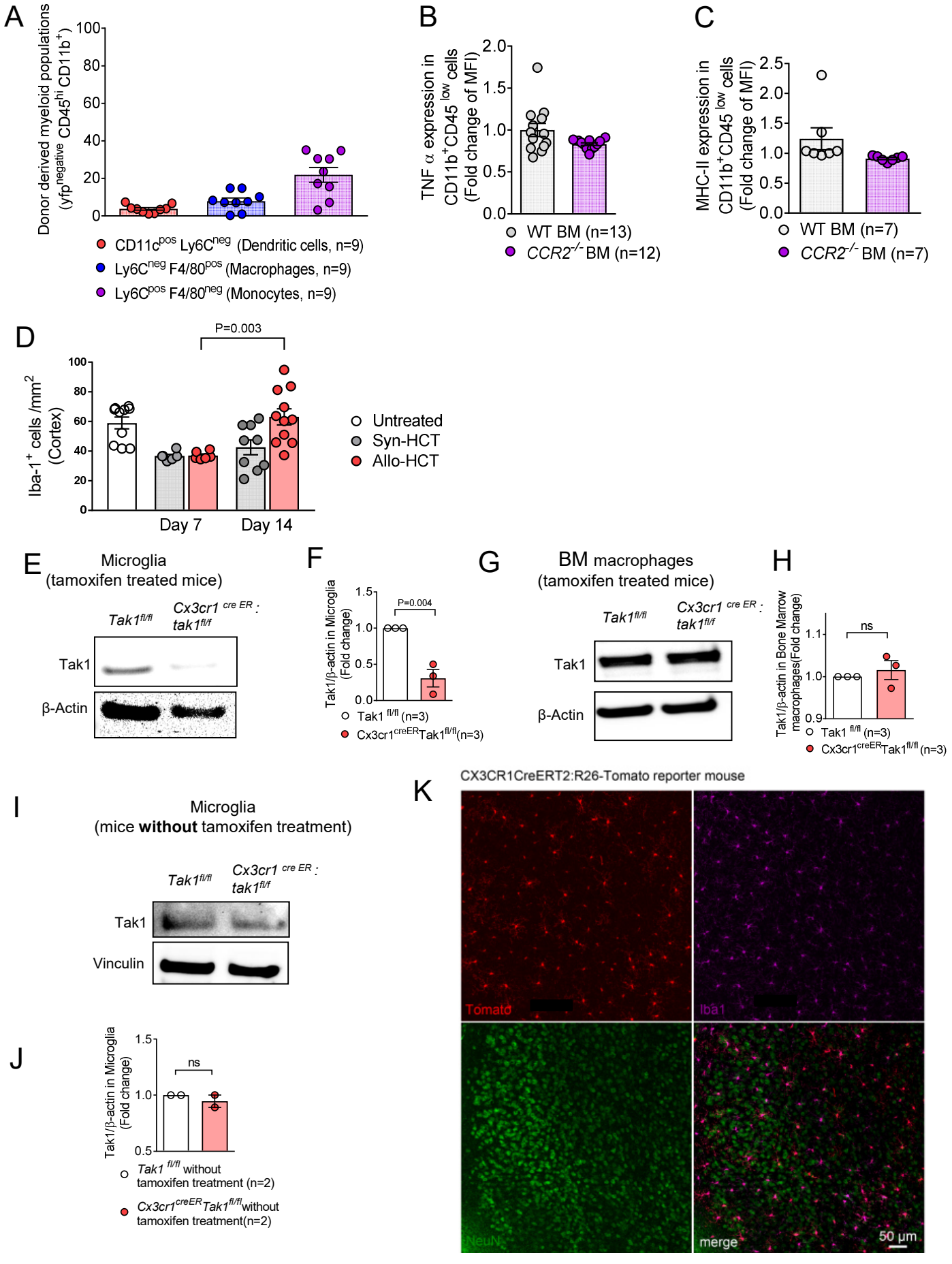

Suppl. Figure 2

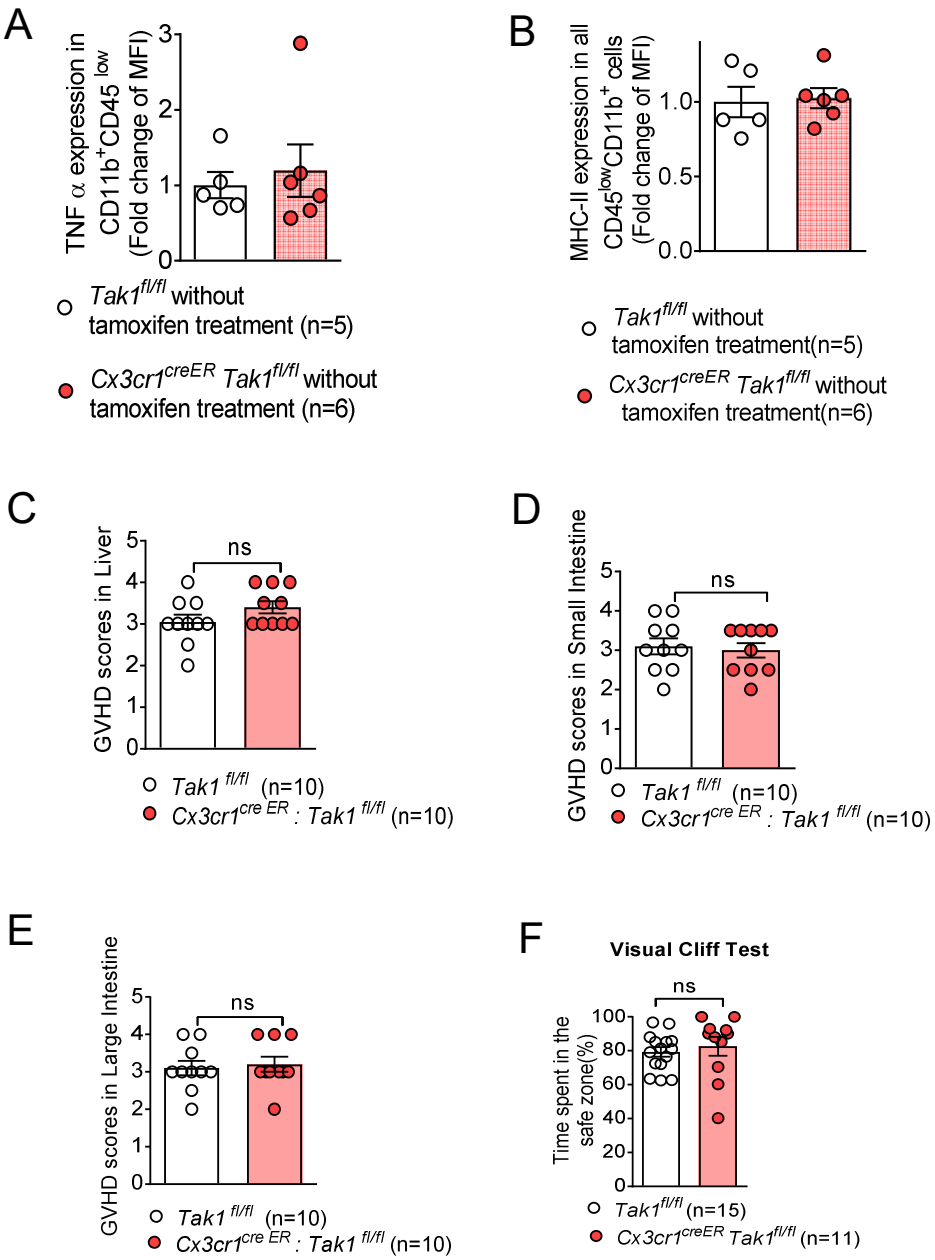

Suppl. Figure 3

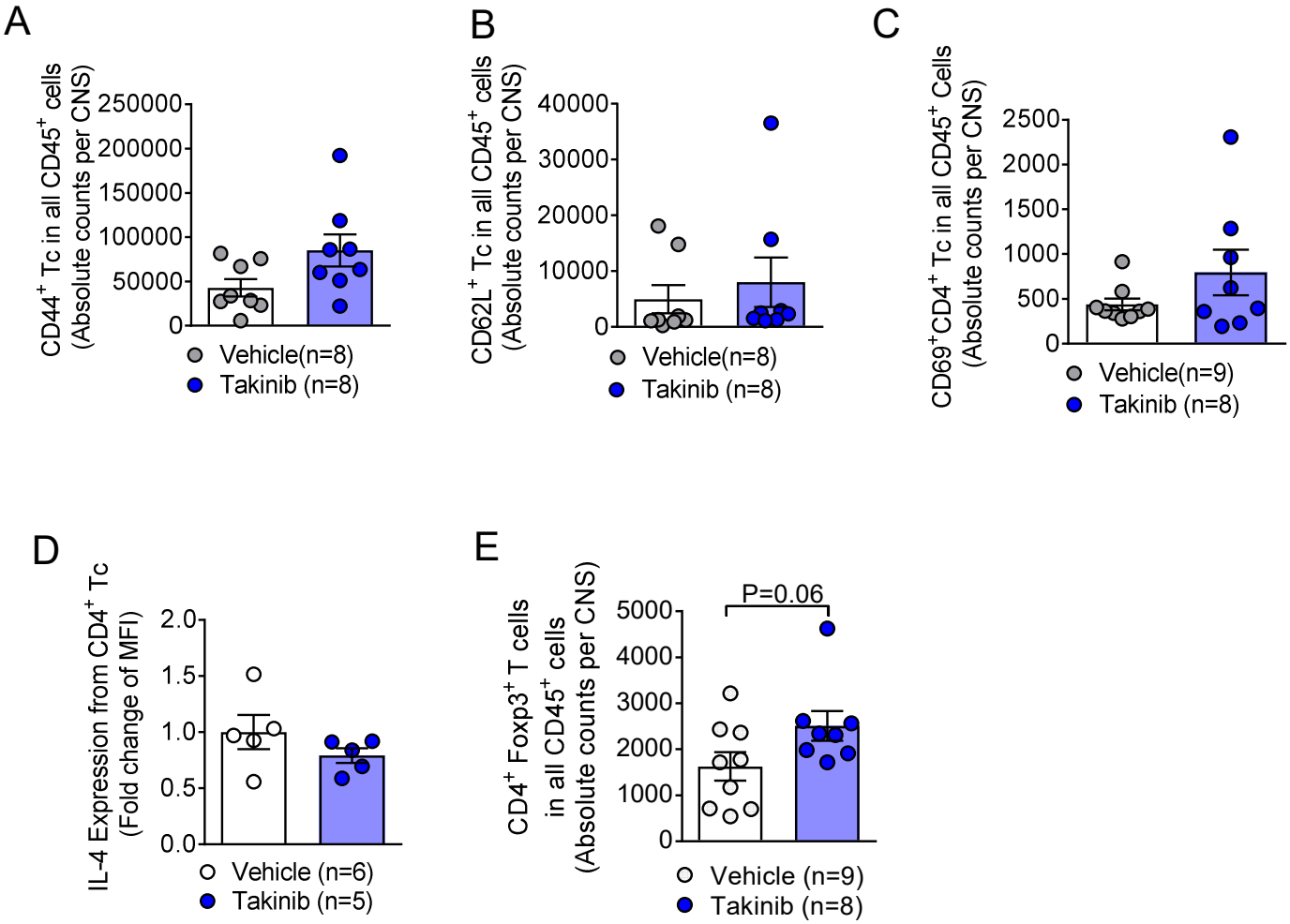

Suppl. Figure 4

A

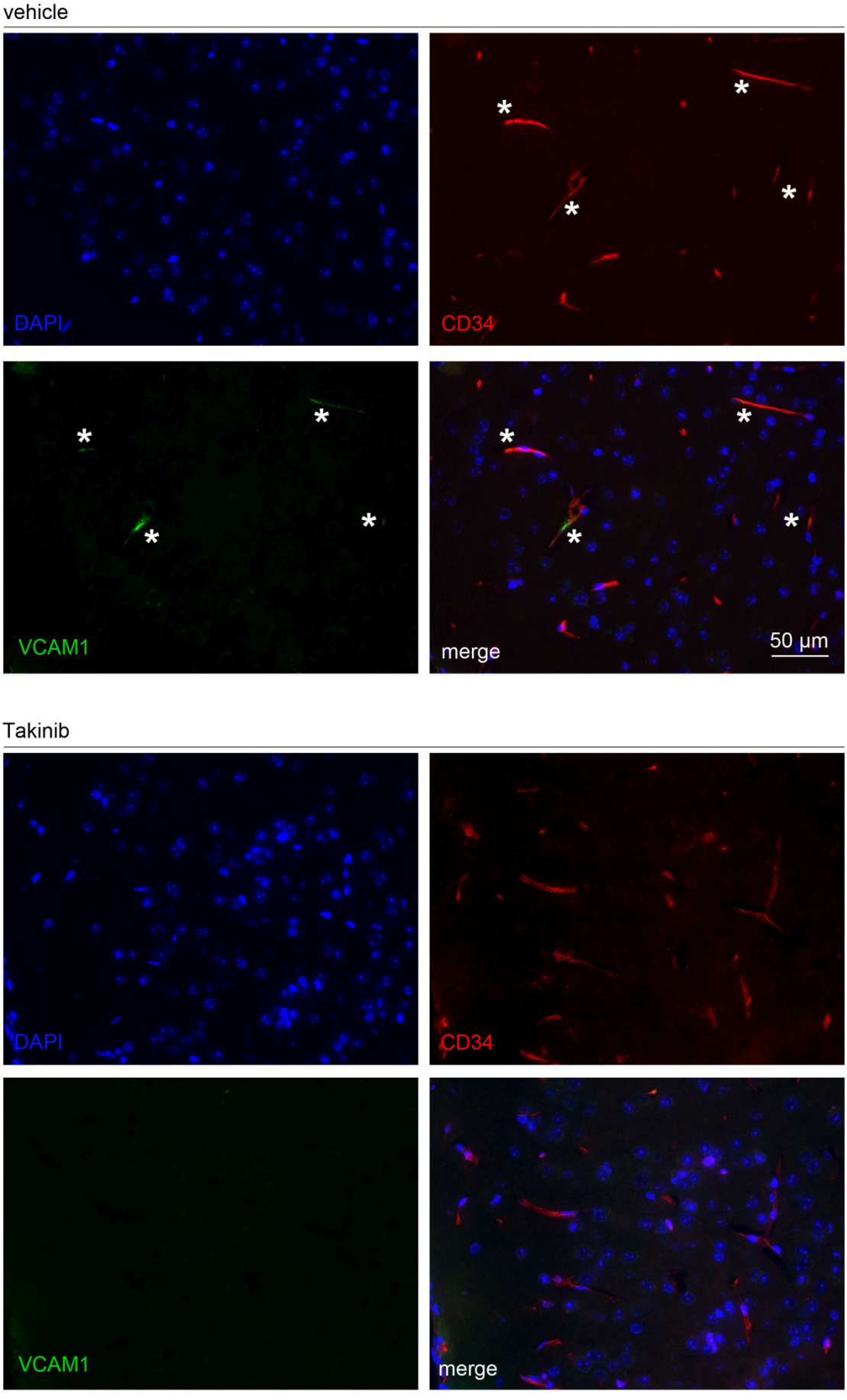

Suppl. Figure 5

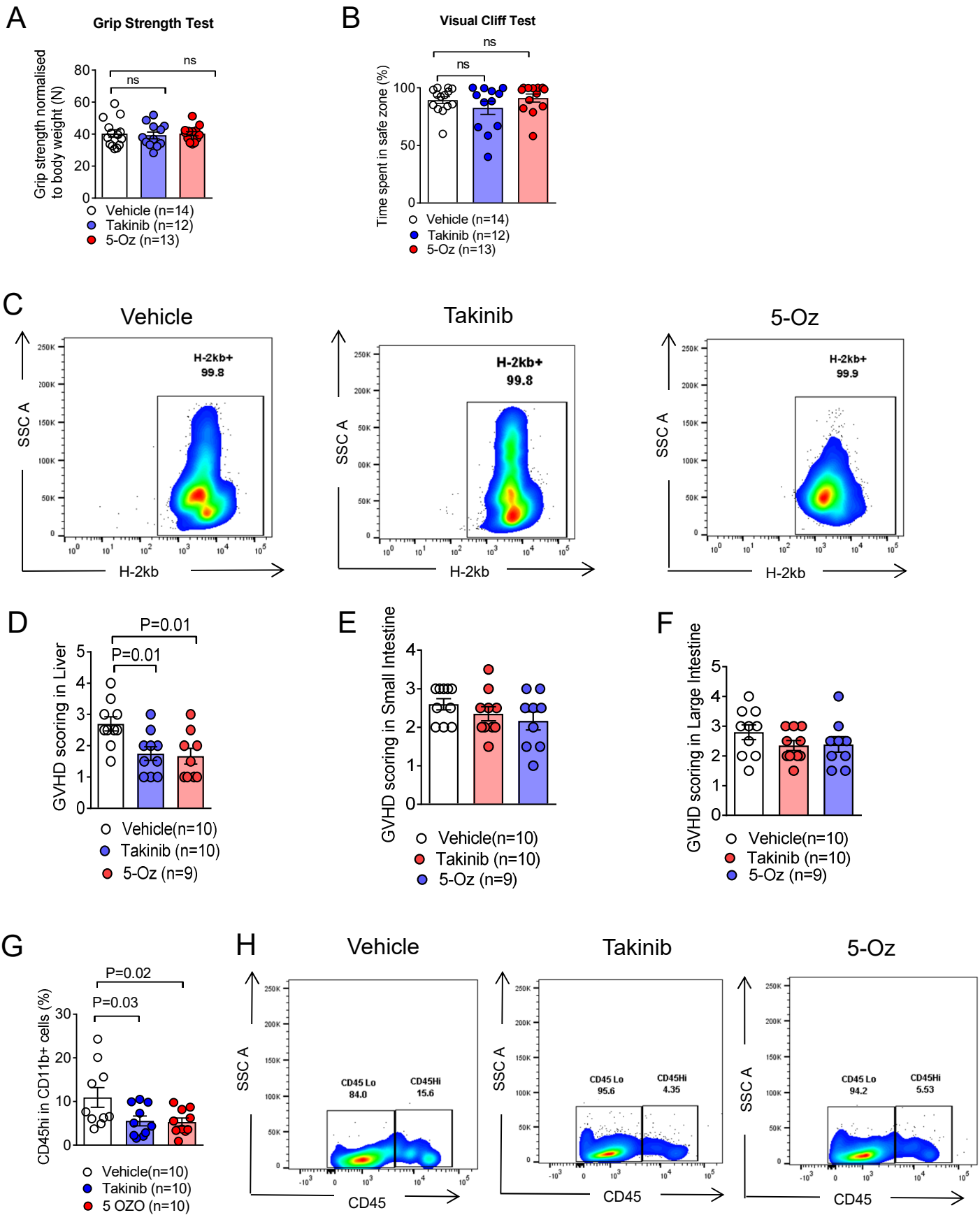

Supplementary Materials and Methods

Suppl. Figure legends

Suppl. Figure S1: Tak1 is deleted in *Cx3cr1^{creER} Tak1$^{fl/fl}$* mice

(A) Flow cytometric characterization of CD45^{hi} cells from CNS. Scatter plot showing the percentages of dendritic cells, macrophages and monocytes in the CD45^{hi} population from the CNS of Cx3cr1$^{cre\ ER}$: R26-yfp mice (n=9) on day 14 after allo-HCT as indicated.

(B) The scatter plot shows the quantification (fold change of MFI) of intracellular TNF expression in microglia from the CNS of BALB/c mice on day 14 after allo-HCT transplanted with either C57BL/6 BM (n=13) or CCR2$^{-/-}$ BM (n=12) as indicated. The experiment was repeated two times and the results (mean ± s.e.m.) were pooled. The *P*-values were calculated using the two-sided Student's unpaired t-test.

(C) The scatter plot shows the quantification (fold change of MFI) of MHC-II expression in microglia from the CNS of BALB/c mice on day 14 after allo-HCT transplanted with either C57BL/6 BM (n=7) or CCR2$^{-/-}$ BM (n=7) as indicated. The experiment was performed once. The *P*-values were calculated using the two-sided Student's unpaired t-test.

(D) The scatter plot shows the number of Iba-1^{+} cells (per mm^2) in cerebral cortex from untreated BALB/c mice or BALB/c mice on day 7 and day 14 after allo-HCT or syn-HCT as indicated. The experiment was repeated two times and the results (mean ± s.e.m.) were pooled. The *P*-values were calculated using one-way ANOVA.

(E-J) Western blot using protein derived from (**e, f**) sorted microglia and (**g, h**) Bone marrow derived macrophages from *Tak1$^{fl/fl}$* (n=3) and *Cx3cr1^{creER} Tak1$^{fl/fl}$* (n=3) mice that had received tamoxifen induction. **(f, h)** Quantification of Tak1 normalized to β-actin (fold change with respect to *Tak1$^{fl/fl}$* controls) in microglia from *Tak1$^{fl/fl}$* and *Cx3cr1^{creER} Tak1$^{fl/fl}$* and Bone marrow macrophages, respectively as indicated. The experiment was repeated two times and the results (mean ± s.e.m.) were pooled. The *P*-values were calculated using the two-sided Student's unpaired t-test

(I, J) Western blot using protein derived from sorted microglia from *Tak1$^{fl/fl}$* (n=2) and *Cx3cr1^{creER} Tak1$^{fl/fl}$* (n=2) mice without tamoxifen induction. **(J)** Quantification of Tak1 normalized to vinculin (fold change with respect to *Tak1$^{fl/fl}$* controls). The experiment was repeated two times and the results (mean ± s.e.m.) were pooled. The *P*-values were calculated using the two-sided two-sided Student's unpaired t-test.

(K) Immunofluorescence images of the CNS of a *Cx3cr1^{creER} R26-Tomato* mouse showing the *Cx3cr1^{creER}: R26*-Tomato reporter system (red), Iba1^{+} microglia (blue) and the neuronal marker NeuN (green). The red *Cx3cr1^{creER}* reporter signal overlays only with blue Iba1^{+} microglia indicating the specificity of the CreER system.

Suppl. Figure S2: TAK1 deletion is specific to microglia in *Cx3cr1^{creER} Tak1$^{fl/fl}$* mice

(A) The scatter plot shows the quantification of intracellular TNF expression (fold change of MFI) on microglia from *Tak1*$^{fl/fl}$ *(n=5)* and *Cx3cr1*^{creER} *Tak1*$^{fl/fl}$ (n=6) vs Tamoxifen treated *Tak1*$^{fl/fl}$ (n=11) and *Cx3cr1*^{creER} *Tak1*$^{fl/fl}$ (n=10) on day 14 after allo-HCT as indicated. The experiment was performed twice. The *P*-values were calculated using the two-sided Student's unpaired t-test.

(B) The scatter plot shows the quantification of MHC-II expression (fold change of MFI) on microglia from *Tak1*$^{fl/fl}$ *(n=5)* and *Cx3cr1*^{creER} *Tak1*$^{fl/fl}$ (n=6) vs Tamoxifen induced *Tak1*$^{fl/fl}$ (n=10) and *Cx3cr1*^{creER} *Tak1*$^{fl/fl}$ (n=11) on day 14 after allo-HCT as indicated. The experiment was performed twice. The *P*-values were calculated using the two-sided Student's unpaired t-test.

(C-E) GVHD histopathology scoring of the liver, small bowel and large bowel from *Tak1*$^{fl/fl}$ (n=10) and *Cx3cr1*^{creER} *Tak1*$^{fl/fl}$ (n=10) mice on day 14 after allo-HCT as indicated. Each data point represents an individual mouse. The experiment was repeated two times and the results (mean ± s.e.m.) were pooled. The *P*-values were calculated using the two-sided Student's unpaired t-test.

(F) The scatter plot shows the percentage of time spent in the safe zone by *Tak1*$^{fl/fl}$ (n=15) and *Cx3cr1*^{creER} *Tak1*$^{fl/fl}$ (n=11) mice on day 14 after allo-HCT. The experiment was repeated three times and the results (mean ± s.e.m.) were pooled. The *P*-values were calculated using the two-sided Student's unpaired t-test.

Suppl. Figure S3: Impact of Tak1 inhibition on T cell subpopulations infiltrating the CNS

(A-E) Flow cytometry analysis of T cell subpopulations in the CNS. **(A)** Scatter plots showing the quantification (in absolute counts per CNS) of **(A)** CD44$^+$ **(B)** CD62L$^+$ and **(C)** CD4$^+$ CD69$^+$ T cells from brains of BALB/c mice treated with vehicle (n=8) or takinib (n=8) on day 14 after allo-HCT as indicated. The experiment was repeated three times and the results (mean ± s.e.m.) were pooled. The *P*-values were calculated using the two-sided Student's unpaired t-test.

(D) The scatter plot shows the quantification of intracellular IL-4 expression (fold change of MFI) in CD4$^+$ T cells from brains of BALB/c mice treated with vehicle (n=6) or takinib (n=5) on day 14 after allo-HCT as indicated. The experiment was repeated two times and the results (mean ± s.e.m.) were pooled. The *P*-values were calculated using the two-sided Student's unpaired t-test.

(E) The scatter plot shows the quantification (in absolute counts per CNS) of CD4$^+$FOXP3$^+$ T cells from CNS of BALB/c mice treated with vehicle (n=9) or takinib (n=8) on day 14 after allo-HCT as indicated. The experiment was repeated three times and the results (mean ±

s.e.m.) were pooled. The *P*-values were calculated using the two-sided Student's unpaired t-test

Suppl. Figure S4: Impact of Tak1 inhibition on VCAM expression in CD34^{+} endothelial cells in the CNS

(A) A representative image from the groups receiving vehicle or takinib, respectively is shown. Scale bars, 50µm.

Suppl. Figure S5: Impact of Tak1 inhibition on CD45^{hi} cells among all CD11b^{+} cells in the CNS

(A) The scatter plot shows the grip strength normalized to body weight (N) of vehicle (n=14), takinib (n=12) and (5*Z*)-7-Oxozeaenol (5-Oz) (n=13) mice on day 14 after allo-HCT in in a grip strength test. The experiment was repeated three times and the results (mean ± s.e.m.) were pooled. The *P*-values were calculated using the one-way ANOVA.

(B) The scatter plot shows the percentage of time spent in the safe zone by BALB/c mice on day 14 after allo-HCT treated with vehicle (n=14), takinib (n=12) or 5 Oz (n=13) as indicated. The experiment was repeated three times and the results (mean ± s.e.m.) were pooled. The *P*-values were calculated using the one-way ANOVA.

(C) Engraftment of donor cells in BALB/c mice on day 30 after BM transplantation treated with vehicle, takinib or 5 Oz as indicated. H-2kb positive cells are donor derived. The experiment was repeated two times with comparable results.

(D-F) GVHD histopathology scoring of the liver, small bowel and large bowel of BALB/c mice on day 14 after allo-HCT treated with vehicle (n=10), takinib (n=10) or 5-Oz (n=9). Each data point represents an individual mouse. The experiment was repeated two times and the results (mean ± s.e.m.) were pooled. The *P*-values were calculated using the one-way ANOVA.

(G, H) Representative flow cytometry analysis and quantification of CD45^{hi} cells among all CD11b^{+} cells in the CNS from BALB/c mice on day 14 after allo-HCT treated with vehicle, takinib or 5-Oz (n=10 in each group) as indicated. **(G)** A representative flow cytometry plot from each group is shown. **(H)** The scatter plot shows the quantification of CD45^{hi} cells among CD11b^{+} cells from different groups as indicated. The experiment was repeated three times and the results (mean ± s.e.m) were pooled. The *P*-values were calculated using the one-way ANOVA.

.

Suppl. Table 1: Control group (no allo-HCT) - Patients characteristics and cause of death

Total number of patients	9
Variable	
	median (range)
Pt. age in years	49 (24-70)
	% (absolute number)
Gender	
female	33.3 (3)
male	66.7 (6)
Cause of death	
Solid tumor	33.3 (3)
Cardiovascular disease	44.5 (4)
Other	22.2 (2)

Abbreviations: Allo-HCT: allogeneic hematopoietic cell transplantation, Pt.: patients

Suppl. Table 2: Patients undergoing allo-HCT - Patients and disease characteristics

Group	Allo-HCT/no GVHD	Allo-HCT/GVHD III-IV°
Pt number	9	10
Variable		
	median (range)	
Pt. age at death (years)	56 (53-72)	51 (25-73)
	% (absolute number)	
Gender		
female	44.4 (4)	40.0 (4)
male	55.6 (5)	60.0 (6)
Disease		
AML/MDS	88.9 (8)	70.0 (7)
Lymphoma	11.1 (1)	0.0 (0)
Multiple myeloma	0 (0)	10.0 (1)
Other	0 (0)	20.0 (2)
Remission status at transplant		
CR	22.2 (2)	40.0 (4)
PR	11.1 (1)	0.0 (0)
Refractory disease	44.5 (4)	60.0 (6)
Relapse	22.2 (2)	0.0 (0)

Abbreviations: Allo-HCT: allogeneic hematopoietic cell transplantation, GVHD: graft-versus-host disease, Pt.: patients, AML: acute myeloid leukemia, MDS: myelodysplastic syndrome, CR: complete remission, PR: partial remission.

Suppl. Table 3: Patients undergoing allo-HCT - Chemotherapy conditioning regimens and transplant characteristics

Group	Allo-HCT/no GVHD	Allo-HCT/GVHD III-IV°
Variable		
	% (absolute number)	
Conditioning regimen		
MAC	22.2 (2)	30.0 (3)
RIC	77.8 (7)	70.0 (7)
Donor type		
MRD	11.1 (1)	10.0 (1)
MUD	55.6 (5)	80.0 (8)
MMUD	33.3 (3)	10.0 (1)
Graft source		
PBSC	88.9 (8)	100.0 (10)
BM	11.1 (1)	0.0 (0)
Immunosuppression		
CNI	100.0 (9)	100.0 (10)
MMF	55.6 (5)	40.0 (4)
MTX	11.1 (1)	40.0 (4)
Campath	44.4 (8)	30.0 (3)
ATG	44.4 (4)	60.0 (6)

Abbreviations: Allo-HCT: allogeneic hematopoietic cell transplantation, GVHD: graft-versus-host disease, MAC: Myeloablative conditioning, RIC: reduced intensity conditioning, MRD: matched related donor, MUD: matched unrelated donor, MMUD: mismatched unrelated donor, PBSC: peripheral blood stem cells, BM: bone marrow, CNI: calcineurin inhibitor (tacrolimus, cyclosporine A), MMF mycophenolate mofetil, MTX: methotrexate, ATG: Anti Thymocyte globulin.

Suppl. Table 4: CNS GVHD cases reported in the literature

CNS GVHD (n = patient number reported)	Histology proven (n)	MRI signs (n)	Main finding of the report	Reference
7	2 (autopsy)	7	CNS-related GvHD is a cause of CNS disorders after allo-HSCT and is associated with a poor prognosis.	(1)
1	1 (biopsy)	1	Although rare, CNS GVHD should be included in the differential diagnosis of CNS lesions in patients after organ transplantation.	(2)
1	1 (biopsy)	1	Neurologic symptoms improved with methylprednisolone pulse	(3)
1	0	1	After intrathecal infusion of methylprednisolone, the clinical symptoms as well as the radiological abnormalities disappeared.	(4)
2	1 (biopsy) 1 (autopsy)	2	Histology showed profound perivascular lymphocytic infiltrates composed predominantly of T-lymphocytes that were of donor origin.	(5)
1	1 (biopsy)	1	Histology showed granulomas around small vessels, containing lymphocytes, histiocytes and giant cells.	(6)
1	1 (autopsy)	1	Angiitis-like syndrome of the CNS neurological manifestation of GVHD.	(7)
1	0	1	Steroid treatment caused an immediate improvement in headaches and functional status.	(8)
1	1 (biopsy)	1	Histologic confirmation of CNS granulomatous angiitis in a patient with GVHD.	(9)

Abbreviations: CNS = central nervous system, MRI = magnetic resonance imaging

Suppl. Table 5: Patients characteristics, study population for neurological complications during GVHD

Characteristic	All Patients	Patients with NCs	Patients without NCs	P Value for a positive correlation with NC
Number of patients	503	174	329	
Age, yrs, median (range)	58 (19-79)	56.5 (21-78)	59 (19-79)	NS
Donor, source, n (%)				
MUD	260 (52)	77 (44)	183 (56)	NS
MMUD	100 (20)	37 (21)	63 (19)	NS
MRD	112 (22)	49 (28)	63 (19)	NS
Mismatched	2 (<1)	0 (0)	2 (1)	NS
Haploidentical	29 (6)	11 (6)	18 (5)	NS
Sex, n (%)				
Male	289 (57)	104 (60)	185 (56)	NS
Female	214 (43)	70 (40)	144 (44)	NS
Diagnosis, n (%)				
AML/MDS	304 (60)	102 (59)	202 (61)	NS
ALL	36 (7)	9 (5)	27 (8)	NS
CML	7 (1)	2 (1)	5 (2)	NS
MPN	39 (8)	17 (10)	22 (7)	NS
NHL	62 (12)	25 (14)	37 (11)	NS
MM	32 (6)	9 (5)	23 (7)	NS
Morbus Hodgkin	6 (1)	5 (3)	1 (<1)	NS
AA	8 (2)	2 (1)	6 (2)	NS
Immune defects	6 (1)	1 (<1)	5 (2)	NS
Biphenotypic leukemia	3 (<1)	2 (1)	1 (<1)	NS
Conditioning regiment, n (%)				
Myeloablative	440 (87)	157 (90)	283 (86)	NS
Reduced intensity	61 (12)	16 (9)	45 (14)	NS
No conditioning	2 (<1)	1 (<1)	1 (<1)	NS
GVHD prophylaxis, n (%)				
CyA + MMF	452 (90)	155 (89)	297 (90)	NS
mTOR inhibitor + MMF	15 (3)	9 (5)	6 (2)	NS
ATG	351 (70)	98 (56)	253 (77)	NS
Post Tx Cyclo	43 (9)	18 (10)	25 (8)	NS
Acute GVHD, n (%)				
Grade 0 to 1	321 (64)	8 (5)	313 (95)	NS
Grade 2 to 4	182 (36)	166 (95)	16 (5)	P<.0001

Abbreviations: NC: neurological complications (excluded: vascular or infectious complications), Allo-HCT: allogeneic hematopoietic cell transplantation, GVHD: graft-versus-host disease, MAC: Myeloablative conditioning, RIC: reduced intensity conditioning, MRD: matched related donor, MUD:

matched unrelated donor, MMUD: mismatched unrelated donor, PBSC: peripheral blood stem cells, BM: bone marrow, CNI: calcineurin inhibitor (tacrolimus, cyclosporine A), MMF mycophenolate mofetil, MTX: methotrexate, ATG: Anti Thymocyte globulin.

Suppl. Table 6: Correlation of neurological (CNS) complications and GVHD II°-IV°

Effect	Odds Ratio	Wald Lower 95% Confidence Limit for Adjusted Odds Ratio	Wald Upper 95% Confidence Limit for Adjusted Odds Ratio	p-value
Acute GVHD 2°-4°	467.141	183.005	>999.999	<.0001
Age ≥ 40	0.692	0.216	2.221	0.5362
GENDER	1.668	0.709	3.925	0.2414
Conditioning regimen	1.842	0.509	6.672	0.3522
donor MMUD vs haplo	0.510	0.068	3.844	0.8401
donor MRD vs haplo	0.598	0.081	4.403	
donor MUD vs haplo	0.790	0.118	5.269	

Suppl. Table 7: Antibodies for flow cytometry

Antibody	Clone	Catalogue number	Flourochrome	Vendor
Anti-mouse CD3	17A2	100220	PECy7	Biolegend
Anti-mouse CD45	30-F11	101132	PerCP-Cy5.5	Biolegend
Anti-mouse CD45	30-F11	103126	PB	Biolegend
Anti-mouse CD80	16-10A1	104708	PE	Biolegend
Anti-mouse CD86	GL-1	105021	PB	Biolegend
Anti-mouse CX3CR1	Polyclonal	FAB5825G	Alexa flour 488	R and D systems
Anti-mouse H-2kb	AF6-88.5.5.3	17-5958	APC	eBioscience
Anti-mouse H-2kb	AF6-88.5	116513	PB	Biolegend
Anti-mouse/human B220	RA3-6B2	103247	BV510	Biolegend
Anti-mouse CD11b	M1/70	25-0112	PE-Cy7	eBioscience
Anti-mouse IL-6	MP5-20F3	12-7061-41	PE	eBioscience
Anti-mouse MHC- II	AMS-32.1	17-5323-82	APC	eBioscience
Anti-mouse NK1.1	PK136	BLD-108737	BV510	Biolegend
Anti-mouse p38 MAPK (pT180/pY182)	36/p38	612565	PE	BD Bioscience
Anti-mouse TNF-α	MP6-XT22	506327	BV421	Biolegend
Anti-Mouse CD31	380	12-0311-81	PE	Biolegend
Anti-Mouse CD105	MJ7/18	120413	APC	eBioscience
Anti-Mouse Vcam-1	429	105722	PB	Biolegend
Anti-Mouse Icam-1	3C4(MIC2/4)	105606	FITC	Biolegend
Anti-Mouse CD44	IM7	103012	APC	Biolegend
Anti- Mouse CD62L	MEL-14	104406	FITC	Biolegend
Anti-Mouse CD3	17A2	100220	PECy7	Biolegend
Anti-Mouse CD3	17A2	100213	PB	Biolegend
Anti-Mouse IL-17A	TC11-18H10.1	506920	PerCP-Cy5.5	Biolegend
Anti-Mouse IL-4	11B11	17-7041-81	APC	eBioscience

Anti-Mouse IFNγ	XMG1.2	12-7311-82 / 81	PE	eBioscience
Anti-Mouse CD4	RM4-5	100531	PB	Biolegend
Anti-Mouse CD4	GK1.5	100406	FITC	Biolegend
Anti-Mouse FOXP3	FJK-16s	17-5773	APC	eBioscience
Anti-Mouse CD69	H1.2F3	11-0691	FITC	eBioscience
Anti-Mouse Ly6C	AL-21	560525	PerCP-Cy5.5	BD Bioscience
Anti-Mouse Ly6G	1A8	560600	APC-Cy7	Biolegend
Anti-Mouse F4/80	BM8	123112	PE-Cy5	Biolegend
Anti-Mouse CD45	30-F11	103114	PECy7	Biolegend
Anti-Mouse CD45	30-F11	103116	APC-Cy7	Biolegend
Anti-Mouse CD45	30-F11	103106	PE	Biolegend
Anti- Mouse CD8a	53-6.7	560182	APC-H7	BD Pharmingen
Anti-Mouse CD4	GK1.5	100434	PerCP-Cy5.5	Biolegend
Anti-Mouse CD11c	N418	117307	PE	Biolegend

Abbreviations: PB: Pacific blue, BV: Brilliant violet, FITC: Fluorescein isothiocyanate, APC: Allophycocyanin, PE: Phycoerythrin, -Cy:-Cyanine, PerCP: Peridinin chlorophyll

Suppl. Material and Methods

Leukemic cell lines

AML (FLT3-ITD/ MLL-PTD) leukemic cells (10) and luciferase transfected WEHI-3B (11) cell lines were used in the study. AML (FLT3-ITD/ MLL-PTD) leukemic cells were provided by Dr. B. R. Blazar (University of Minnesota). All the cell lines which were used for *in vivo* experiments were authenticated at DSMZ or Multiplexion, Germany. The murine cell lines were authenticated by COI species analysis to trace them back to their donor mouse strains. All the cell lines were tested repeatedly for Mycoplasma contamination and were found to be negative.

Treatment with inhibitors

Mice were treated with either takinib (Selleckchem, Germany) or 5Z-7-Oxozeaenol (5-Oz) (Sigma-Aldrich, Germany) after allo-HCT. For the treatment with takinib and 5-Oz, a stock solution of 3 mg/ml and 1 mg/ml respectively was prepared in DMSO. The stocks were diluted in 0.5% carboxymethylcellulose solution (vehicle) and was administrated by intraperitoneal injection at a dosage of 0.75 mg/kg (takinib) or 0.25 mg/kg (5-OZ) of mouse per day from day 3 to day 13 following allo-HCT as described previously (12). An equal volume of corresponding vehicles was administrated to the control groups weekly until day 14.

Treatment with tamoxifen

Tamoxifen (T5648, Sigma Aldrich, Germany) was dissolved in corn oil (Sigma Aldrich) by incubation at 42°C for 6 hours. Four milligram of tamoxifen was administrated subcutaneously to the *Cx3cr1*^{CreER} *:Tak1*$^{fl/fl}$ *or Cx3cr1*^{creER}*: R26*-Tomato reporter or *Cx3cr1*^{creER}*: R26-yfp mice* on two days, 48 hours apart as previously described (13). When indicated the mice were not treated with tamoxifen. We treated the *Cx3cr1*^{CreER} *Tnf*$^{fl/-}$ mice with tamoxifen by oral gavage (4x 5mg doses in total). The BM transplantation experiments were performed one month after tamoxifen induced *cre-loxP* recombination.

Graft Versus Leukemia models

AML (WEHI-3B) Model

BALB/c recipients were exposed to lethal irradiation of 9 Gy in equally split doses and were transplanted intravenously with 10,000 AML (WEHI-3B) cells and $5x10^6$ C57BL/6 BM. Two days post transplantation, $3x10^5$ T cells from C57BL/6 mice were administered to induce the

GVL effect. The mice were treated either with takinib / vehicle via intraperitoneal injection at a dosage of 0.75mg per mouse per day from day 3 until day 13.

AML (MLL-PTD FLT3-ITD) leukemia model

For the AML (MLL-PTD FLT3-ITD) leukemia model (10, 14) C57BL/6 recipients were lethally irradiated with 11 Gy split into two equal doses and transplanted with $5x10^6$ BALB/c BM and 5000 AML (MLL-PTD FLT3-ITD) cells. On day 2 post transplantation $5x10^5$ BALB/c splenic T-cells were transplanted. The mice were treated either with takinib / vehicle via intraperitoneal injection at a dosage of 0.75mg per mouse per day from day 3 until day 13.

Transplantation with *CCR2*$^{-/-}$ BM

BALB/c recipients were head shielded and lethally irradiated at a dosage of 9 Gy split exactly into two equal doses. The recipients were transplanted intravenously with $5x10^6$ BM cells either from *CCR2*$^{-/-}$ or WT BM cells along with $3x10^5$ Tc from the C57BL/6 mice. The brains were extracted and analyzed on day 14.

Novel object recognition test

Novel object recognition test was performed as described previously with modifications (15). During the habituation phase, each mouse was allowed to explore two similar objects within a total exploration time of 20s. We commenced the testing phase six hours after the habituation phase. During the testing session, each mouse was allowed to explore a familiar object and a novel object of different shape and texture. The position of the novel object and the familiar object was randomized between each mouse. The time spent by each mouse to explore the novel object and the familiar object was noted. The experiment was stopped when the total exploration time reached 20s. The amount of time spent by the mouse exploring the novel object to the total exploration time is calculated as an index of recognition memory.

Grip strength test

The grip strength test was performed as described previously (16) to assess the fore limb strength of the mice. Each mouse was allowed to grasp on to the metal grid of the apparatus and tail was pulled backwards until they leave the grid. A total of five trials were performed with each mouse and the average of grip strength (N) normalized to the body weight of mouse was estimated.

Elevated plus maze test

We performed the elevated plus maze test to evaluate the anxiety behaviour in mice as described previously with minor modifications (17). Each mouse was kept at the junction of closed arms and open arms of the maze. An open arm entry was considered when the mouse extended its head towards the open arm or when it entered the arm. We quantified the time they spent in the open arm in minutes. This time was then put into relation to the total time frame of six minutes. The resulting value was a percentage showing entry into open arms in relation to the total time.

Visual cliff test

The visual cliff test was employed as described previously(18) with modifications to evaluate the mice's depth perception. The test was conducted for 10 min per mouse. The amount of time spent by the mice in the shallow zone (safe zone) in relation to the total time was calculated.

Isolation of cells from the murine brain

The brain cells were isolated as described previously (19) with modifications. Briefly, the mice were anesthetized and were perfused with 1X cold PBS. The brains were isolated, homogenized and filtered through a 70 µm nylon filter. The homogenate was suspended in 37% isotonic Percoll solution and centrifuged at 800 xg for 30 min without applying break. The myelin layer was removed from the top of 37% Percoll and the pelleted cells were washed with 1X PBS for further analysis.

Isolation of Endothelial cells from murine brain

Briefly, the mice were anesthetized and were perfused with 1X cold PBS. The brains were rolled gently over a Whatmann filter paper to separate the meninges. The brains were homogenized and incubated at 37°C for 30 min in digestion media (Collagenase/Dispase (0.5mg/ml), DNase (0.02mg/ml)). The CNS homogenate was filtered through a 70 µm nylon filter and was suspended in 37% isotonic Percoll solution and centrifuged at 800 xg for 30 min without applying break. The myelin layer was removed from the top of 37% Percoll and the pelleted cells were washed with 1X PBS for further analysis.

Primary microglia culture

Primary microglial cultures were performed as per the method described earlier with minor modifications (20). Microglia were treated with different concentrations of murine TNF-α (Peprotech, Germany) for 24h and was lysed for western blotting as described below.

Western Blotting

The cells were lysed using a radio-immunoprecipitation assay buffer (Santa Cruz Biotechnology, Heidelberg, Germany) supplemented with Phosphatase Inhibitor Cocktail 2 (Sigma-Aldrich, Germany). The protein concentration was determined using Pierce™ BCA Protein Assay Kit (Life Technologies, Germany). The protein samples were transferred onto nitrocellulose membranes (Amersham Biosciences, Germany) after running and resolving the total proteins in 4% to 12% sodium dodecyl sulphate-polyacrylamide electrophoresis gels (NuPAGE, Invitrogen, Germany). The membrane was incubated with blocking buffer (5% BSA in 1X tris buffer saline containing 0.1% tween-20) followed by incubation with primary antibodies diluted in blocking buffer. All antibodies used in our study were purchased from Cell Signaling Technology, USA or Santacruz Biotechnology, USA. The primary antibodies used were anti-mouse TAK1 (catalog no: 4505, polyclonal)(21), anti-mouse phospho TAK1 (Ser412) (catalog no: 9339, polyclonal)(22), anti-mouse β-actin (catalog no: 4970, clone: 13E5)(23), anti-mouse NF-KB p65 (catalog no: 8242, polyclonal)(24), anti-mouse phospho NF-KB p65 (Ser536) (catalog no: 3033, clone: N3H1), anti-mouse JNK (catalog no: 9252, polyclonal), anti-mouse Phospho-SAPK/JNK (Thr183/Tyr185) (Catalog no : 9255, Clone : G99), anti-Mouse Vinculin(sc73614, 7F9). Anti-rabbit IgG, HRP-linked Antibody (catalog no: 7074) and Anti-Mouse IgG, HRP-linked Antibody (catalog no: 7076) were used as the secondary antibodies. WesternBright Sirius Chemiluminescent Detection Kit (Advansta, USA) was used as the chemoluminescent substrate. The signals from the blot are captured using the ChemoCam Imager 3.2 (Intas Science Imaging Instruments GmbH, Germany) and quantified using LabImage 1D software.

Immunohistochemistry for CD3 and Iba-1

The mice were deeply anesthetized and killed by perfusing them with cold PBS on day 14 of transplantation. The brains were removed, fixed in buffered formalin and embedded in paraffin. The tissues were sectioned and deparaffinized. Antigen retrieval was achieved by citrate buffer (pH=6) treatment for 40 min. Endogenous peroxidases were blocked with 3%H_2O_2. The sections were stained with rabbit anti-Iba-1 (catalog no: 012-26723, clone: NCNP24, 1:500, Wako) and rat anti-CD3 (catalog no: MCA1477, clone: CD3-12, 1:100, Bio Rad) antibodies separately for identifying myeloid cells and T-cells respectively. The sections were then incubated with biotinylated secondary antibody anti-rabbit (1:200) for Iba-1 and anti-rat (1:200) for CD3. The paraffin-embedded patient-derived brain tissues were sectioned and stained similarly for Iba-1^+ cells. We used mouse anti-human CD3 (catalog no: NCL-L-CD3-565, clone: LN10, Leica Biosystems, 1:50) for human $CD3^+$ staining.

Immunofluorescence for TNFα in human brain biopsies

FFPE sections from brain tissue were stained with anti-Iba-1 (cat. no. 019-19741, Wako) and anti-TNFa (cat. no. ab1793, Abcam) antibodies overnight (Iba-1: dilution 1:500; Anti-TNFa: dilution 1:50 at 4 °C), followed by Alexa Fluor 488–conjugated secondary goat-anti-rabbit antibody (cat. no. A11034, ThermoFisher) and Alexa Fluor 568–conjugated goat-anti-mouse secondary antibody (cat. no. A11004, ThermoFisher) staining, which was added at a dilution of 1:500 respectively for 2 hours at room temperature. Nuclei were counterstained with DAPI. Afterwards, autofluorescence was reduced by TrueBlack® Lipofuscin Autofluorescence Quencher (cat. no. 23007) and applied for 5 minutes followed by three washing steps with 1x PBS.

Immunofluorescence for Vcam-1 in endothelial cells

FFPE sections from brain tissue were stained with Anti-VCAM-1 (cat.no .134047, Abcam), Anti-CD34 (cat. no. C47878, LS Bio) antibodies overnight (Anti-VCAM-1:500; Anti-CD34 1:100 at 4 °C) followed by Alexa Fluor 488–conjugated secondary goat-anti-rabbit antibody (cat. no. A11034, ThermoFisher) and Alexa Fluor 568–conjugated goat-anti-rat secondary antibody (cat. no. A11077, ThermoFisher) staining which was added at a dilution of 1:500 respectively for 2 hours at room temperature. Nuclei were counterstained with DAPI.

Immunofluorescence staining for NeuN and Iba-1 in reporter mouse

Cryo sections from brain tissue of tamoxifen treated *Cx3cr1*^{creER}*:R26* tomato reporter mice were stained with Anti-Iba-1 (Ab139590, Abcam), Anti-NeuN (cat. no. MAB377,Millipore) antibodies overnight (Anti-Iba-1 -1:1000; Anti-NeuN 1:100) at 4 °C) followed by Alexa Fluor 568–conjugated goat-anti-rabbit secondary antibody (cat. no A-11011, ThermoFisher) and Alexa Fluor 488–conjugated secondary goat-anti-mouse antibody (A-21042, ThermoFisher) staining which was added at a dilution of 1:500 respectively for 2 hours at room temperature. Nuclei were counterstained with DAPI.

RNA sequencing

Analyses performed in Freiburg on WT mice:

Microglia cells were sorted in a BD FACSAria fusion or BD FACSAria III (BD Biosciences, Germany) cell sorter through a 85 µm nozzle. RNA was isolated using PicoPure™ RNA Isolation Kit (ThermoFischer Scientific, Germany) followed by library preparation according to manufacturer's instructions for low input RNA sequencing.

RNA was paired-end sequenced on an Illumina HiSeq4000 at the Genome and Proteome Core Facility (GPCF) of the German Cancer Research Center (DKFZ, Heidelberg, Germany). In total 4 replicates were analyzed for each group: untreated, Syn-HCT and Allo-HCT. On average, $5.23*10^7$ reads were filtered-in after adapter-trimming and bad quality reads

removal using Trimmomatic (25). Alignment and read count per gene were done by STAR (26). An average of $4.55*10^7$ reads (87%) was uniquely aligned to the mouse genome (mm9). The downstream analysis was performed with DESeq2 R package (27). Differentially regulated genes between Allo-HCT and Sync-HCT were selected based on an adjusted p-value threshold bellow 0.05 (Benjamini-Hochberg false discovery rate correction).
For raw data see GEO accession GSE141663:
Go to https://www.ncbi.nlm.nih.gov/geo/query/acc.cgi?acc=GSE141663
Enter token mjsdsqikzpihxqj into the box

Analyses performed at the Weizmann institute of Science on *Tnf*$^{fl/-}$ and *Cx3cr1*^{CreER}*:Tnf*$^{fl/-}$ mice:

EC mRNA sequencing was conducted with the help of the INCPM unit at the Weizmann institute of Science – total RNA was extracted from $0.1\text{-}1*10^6$ sorted cells with RNeasy Micro Kit (Qiagen). 100 ng of total RNA was processed using the TruSeq Stranded Total RNA HTSample Prep Kit (with Ribo-Zero Gold) of Illumina (RS-122-2303). Libraries were evaluated by Qubit and TapeStation. Sequencing libraries were constructed with barcodes to allow multiplexing of 24 samples ran on 3 lanes. ~20 million single-end 50-bp reads were sequenced per sample on Illumina HiSeq 2500 high output mode instrument.
Macrophage mRNA was sequenced using MARSeq, as previously described (28). Briefly, 10^4–10^5 cells from each population were sorted into 50 µl of lysis/binding buffer (Life Technologies). mRNA was captured with 15 µl of Dynabeads oligo(dT) (Life Technologies), washed, and eluted at 85°C with 6 µl of 10 mM Tris-Cl (pH 7.5). ~5 million reads were sequenced per library. In both cases gene expression levels were calculated using the HOMER software package (analyzeRepeats.pl rna mm9 -d <tagDir> -count exons -condenseGenes -strand + -raw) (29). Normalization and differential expression analysis was done using the DESeq2 R-package,

Flow cytometry

All antibodies used for flow cytometry are listed in Suppl. Table 4. For all fluorochrome-conjugated antibodies, optimal concentrations were determined using titration experiments. Cells were incubated with the respective antibodies diluted in FACS buffer for 20 minutes at 4°C for surface antigen staining. Cells were then washed with FACS buffer according to the manufacturer's instruction For murine p38 MAPK expression analysis, cells were fixed with one part pre-warmed 3.7% formalin and one part FACS buffer; and then exposed to 90% methanol, before application of the p38 MAPK antibody. All intracellular cytokine stainings

were performed using BD Cytofix/Cytoperm kit (BD Biosciences, Germany) according to manufacturer's instruction. For intracellular cytokine staining for murine TNF-α, IL-6, IL-1β,IL-17 and IFNγ cells were treated with 1 µl/ml media of Brefeldin A (Golgi Plug, BD Biosciences, Germany) for 4 hours prior to staining. Foxp3 staining was performed using ebioscience transcription factor staining kit (eBiosciences, Germany) according to the manufacturer's instructions. For excluding dead cells, the live/dead fixable dead cell stain kit from Molecular Probes, USA was used according to the manufacturer's instructions. Data was acquired on the BD LSR Fortessa (BD Biosciences, Germany) and analyzed using Flow Jo software (Tree Star, USA).

3-D reconstruction using Imaris

The brains were removed on day 14 after transplantation and fixed in 4% paraformaldehyde. The tissues were embedded in paraffin prior to the analysis. Thick sections of 30µM were stained with Rabbit Iba-1 antibody (019-19741, Wako, Japan) for 72 h followed by a goat anti-rabbit Alexa Flour 568 or goat anti-rabbit 647 (A21246, ThermoFischer Scientific, Germany) secondary antibody for 48h. The nuclei were counter stained with DAPI . Images were procured in Olympus Fluoview 1000 confocal laser scanning microscope as described previously (13). The microglia was reconstructed using the Imaris software (Bitplane).

References:

1. Ruggiu M, Cuccuini, W., Mokhtari K, Meignin V, Peffault de Latour R, Robin M, Fontbrune FS, Xhaard A, Socié G, Michonneau D. Case report: Central nervous system involvement of human graft versus host disease: Report of 7 cases and a review of literature. *Medicine (Baltimore).* 2017;96(e8303.
2. Saad AG, Alyea, E.P., Wen PY, DeGirolami U, Kesari S. Graft-Versus-Host Disease of the CNS After Allogeneic Bone Marrow Transplantation. *J Clin Oncol.* 2009;27(147-9.
3. Min GJ, Park S, Park SS, Yoon JH, Lee SE, Cho BS, Eom KS, Lee S, Kim HJ, Min CK, Cho SG, Kim DW, Lee JW, Kim YJ. A case of central nervous system graft-versus-host disease following allogeneic stem cell transplantation. *Int J Hematol.* 2019;110(635-9.
4. Polchlopek Blasiak K, Simonetta, F., Vargas MI, Chalandon, Y. Central nervous system graft-versus-host disease (CNS-GvHD) after allogeneic haematopoietic stem cell transplantation. *BMJ Case Rep.* 2018;doi: 10.1136/bcr-2017-221840(
5. Kamble RT, Chang CC, Sanchez S, Carrum G. Central nervous system graft-versus-host disease: report of two cases and literature review. *Bone Marrow Transplant.* 2007;39(49-52.
6. Kew AK, Macaulay, R., Burrell S, Rubin S, Dow G, Couban S. Central nervous system graft-versus-host disease presenting with granulomatous encephalitis. *Bone Marrow Transplant.* 2007;40(183-4.
7. Padovan CS, Bise, K., Hahn, J., Sostak P, Holler E, Kolb HJ, Straube A. Angiitis of the central nervous system after allogeneic bone marrow transplantation? *Stroke.* 1999;30(1651-6.
8. Shortt J, Hutton, E., Faragher M, Spencer A. Central nervous system graft-versus-host disease post allogeneic stem cell transplant. *Br J Haematol.* 2006;132(245-7.

9. Ma M, Barnes, G., Pulliam, J., Jezek, D., Baumann, R. & Berger, J. CNS angiitis in graft vs host disease. *Neurology.* 2002;59(1994-97.
10. Bernot KM, Nemer, J.S., Santhanam, R., Liu, S., Zorko, N.A., Whitman, S.P., et al. Eradicating acute myeloid leukemia in a Mll(PTD/wt):Flt3(ITD/wt) murine model: a path to novel therapeutic approaches for human disease. *Blood.* 2013;122(3778-83.
11. Warner NL, Moore, M.A., Metcalf, D. A transplantable myelomonocytic leukemia in BALB-c mice: cytology, karyotype, and muramidase content. *Journal of the National Cancer Institute.* 1969;43(963-82.
12. Kobayashi A, Kobayashi, S., Miyai, K., Osawa, Y., Horiuchi, T., Kato, S., et al. TAK1 inhibition ameliorates survival from graft-versus-host disease in an allogeneic murine marrow transplantation model. *Int J Hematol.* 2018;107(222-9.
13. Goldmann T, Wieghofer, P., Jordão, M.J., Prutek, F., Hagemeyer, N., Frenzel, K., et al. Origin, fate and dynamics of macrophages at central nervous system interfaces. *Nat Immunol.* 2016;17(797-805.
14. Zorko NA, Bernot, K.M., Whitman, S.P., Siebenaler, R.F., Ahmed, E.H., Marcucci, G.G., Yanes, D.A., McConnell, K.K., Mao, C., Kalu, C., Zhang, X., Jarjoura, D., Dorrance, A.M., Heerema, N.A., Lee, B.H., Huang, G., Marcucci, G., Caligiuri, M.A. Mll partial tandem duplication and Flt3 internal tandem duplication in a double knock-in mouse recapitulates features of counterpart human acute myeloid leukemias. *Blood.* 2012;120(1130-6.
15. Leger M, Quiedeville, A., Bouet, V., Haelewyn B, Boulouard M, Schumann-Bard P, Freret T. Object recognition test in mice. *Nat Protoc.* 2013;12(2531-7.
16. Abbas MG, Shoji, H., Soya, S., Hondo, M., Miyakawa, T., Sakurai, T. Comprehensive Behavioral Analysis of Male Ox1r (-/-) Mice Showed Implication of Orexin Receptor-1 in Mood, Anxiety, and Social Behavior. *Front Behav Neurosci.* 2015;9(324.
17. Walf AA, Frye, C.A. The use of the elevated plus maze as an assay of anxiety-related behavior in rodents. *Nat Protoc.* 2007;2(322-8.
18. Mazziotti R, Baroncelli, L., Ceglia, N., Chelini, G., Sala, G.D., Magnan, C., et al. Mir-132/212 is required for maturation of binocular matching of orientation preference and depth perception. *Nat Commun.* 2017;8(15488.
19. van Loo G, De Lorenzi, R., Schmidt, H., Huth, M., Mildner, A., Schmidt-Supprian, M., Lassmann, H., Prinz, M.R., Pasparakis, M. Inhibition of transcription factor NF-kappaB in the central nervous system ameliorates autoimmune encephalomyelitis in mice. *Nat Immunol.* 2006;7(954-61.
20. Moussaud S, Draheim, H.J. A new method to isolate microglia from adult mice and culture them for an extended period of time. *J Neurosci Methods.* 2010;187(243-53.
21. Ma S, Yang, L.L., Niu, T., et al. SKLB-677, an FLT3 and Wnt/β-catenin signaling inhibitor, displays potent activity in models of FLT3-driven AML. *Sci Rep.* 2015;5(15646.
22. Thedieck K, Holzwarth, B., Prentzell, M.T., et al. Inhibition of mTORC1 by astrin and stress granules prevents apoptosis in cancer cells. *Cell.* 2013;154(859-74.
23. Ippagunta SK, Malireddi, R.K., Shaw, P.J., et al. The inflammasome adaptor ASC regulates the function of adaptive immune cells by controlling Dock2-mediated Rac activation and actin polymerization. *Nat Immunol.* 2011;12(1010-6.
24. Bergstrøm B, Aune, M.H., Awuh, J.A., et al. TLR8 Senses Staphylococcus aureus RNA in Human Primary Monocytes and Macrophages and Induces IFN-β Production via a TAK1-IKKβ-IRF5 Signaling Pathway. *J Immunol.* 2015;195(1100-11.
25. Bolger AM, Lohse, M., Usadel, B. Trimmomatic: a flexible trimmer for Illumina sequence data. *Bioinformatics (Oxford, England).* 2014;30(2114-20.
26. Dobin A, Davis, C.A., Schlesinger F, Drenkow J, Zaleski C, Jha S, Batut P, Chaisson M, Gingeras TR. STAR: ultrafast universal RNA-seq aligner. *Bioinformatics (Oxford, England).* 2013;29(15-21.
27. Love MI, Huber W, Anders S. Moderated estimation of fold change and dispersion for RNA-seq data with DESeq2. *Genome biology.* 2014;15(550.

28. Jaitin DA, Kenigsberg, E., Keren-Shaul, H., Elefant N, Paul F, Zaretsky I, Mildner A, Cohen N, Jung S, Tanay A, Amit I. Massively parallel single-cell RNA-seq for marker-free decomposition of tissues into cell types. *Science.* 2014;343(776-9.
29. Heinz S, Benner, C., Spann, N., Bertolino E, Lin YC, Laslo P, Cheng JX, Murre C, Singh H, Glass CK. Simple combinations of lineage-determining transcription factors prime cis-regulatory elements required for macrophage and B cell identities. *Mol Cell.* 2010;38(576-89.